

# Comparison of Mass Transfer Characteristics between Countercurrent-Flow and Crosscurrent-Flow Rotating Packed Bed

Qi Guisheng<sup>1,2</sup>; Guo Linya<sup>1,2</sup>; Liu Youzhi<sup>1,2</sup>; Zhang Dongming<sup>1,2</sup>

(1. Research Center of Shanxi Province for High Gravity Chemical Engineering and Technology, North University of China, Taiyuan 030051;

2. Shanxi Province Key Laboratory of Hige-Oriented Chemical Engineering, Taiyuan 030051)

**Abstract:** The rotating packed bed (RPB), mainly including the countercurrent-flow RPB (Counter-RPB) and the crosscurrent-flow RPB (Cross-RPB) that are classified from the perspective of gas-liquid contact style, is a novel process intensification device. A significant measurement standard for evaluating the performance of RPB is the mass transfer effect. In order to compare the mass transfer characteristics of Counter-RPB and Cross-RPB with the same size, the liquid volumetric mass transfer coefficient ( $k_L a_e$ ) and effective interfacial area ( $a_e$ ) were measured under identical operating conditions. Meanwhile, the comparison of comprehensive mass transfer performance was conducted using the ratio of  $\Delta P$  (pressure drop) to  $k_L a_e$  as the standard. Experimental results indicated that  $k_L a_e$  and  $a_e$  increased with the increase in liquid spray density  $q$ , gas velocity  $u$ , and high gravity factor  $\beta$ . Furthermore, compared with the Cross-RPB, the Counter-RPB has higher liquid volumetric mass transfer coefficient and slightly larger effective interfacial area. The experimental results of comprehensive mass transfer performance showed that the Counter-RPB had higher  $\Delta P/k_L a_e$  than the Cross-RPB with changes in liquid spray density and high gravity factor, and there exists a turning point at 0.71 m/s accompanied by a variation with gas velocity. Moreover, the relative error of experimental value to calculated value, which was computed by the correlative expressions of  $k_L a_e$ , was less than 5 %. In conclusion, the mass transfer characteristics of RPB are deeply impacted by the manner in which the flows are established and the Cross-RPB would have a great potential for industrial scale-up applications.

**Key words:** rotating packed bed; mass transfer; crosscurrent-flow; countercurrent-flow; process intensification

## 1 Introduction

High gravity technology is a typical process intensification technology. Since its birth, this technology has been playing a significant role in environmental protection and energy saving, such as CO<sub>2</sub> emission control<sup>[1-4]</sup>, H<sub>2</sub>S absorption process<sup>[5]</sup>, SO<sub>2</sub> removal<sup>[6]</sup>, VOCs removal from waste gas streams<sup>[7-8]</sup>, and wastewater treatment<sup>[9-12]</sup>. High gravity technology is achieved by means of a mass transfer equipment—rotating packed bed<sup>[13]</sup>, in which the packing presents a state of high-speed rotation driven by a rotator. Accordingly, compared with the traditional mass transfer equipment, the liquid could be broken down into numerous smaller droplets, filaments, and films under the action of centrifugal force generated with the rotated packing. Finally, the gas-liquid contact area increases. In conclusion, 2—3 orders of magnitude of enhancement in liquid volumetric mass transfer coefficient can be achieved<sup>[14-16]</sup>

and the average height of transfer units can typically be a few centimeters<sup>[17]</sup>. Besides, the RPB could be operated at higher gas and/or liquid flow rates because of the low tendency of flooding compared to that in the conventional packed bed<sup>[18]</sup>. As a result, the size of equipment would be reduced dramatically. Thereby the capital and operating costs could decrease<sup>[19]</sup>, which would be transformed into competitive advantage in commercial application.

Stankiewicz<sup>[20]</sup> neatly highlighted the fact that a growing world-wide competition would necessitate major changes in the ways by which mass transfer devices are designed. Up to now, there have been three design concepts of the RPB due to different patterns of gas-liquid contact, viz.: the countercurrent-flow RPB (Counter-RPB), the crosscurrent-flow RPB (Cross-

**Received date:** 2019-02-25; **Accepted date:** 2019-04-30.

**Corresponding Author:** Professor Qi Guisheng, E-mail: zbdx-qgs@136.com; Telephone: +86-351-3921986.

RPB), and the concurrent-flow RPB (Con-RPB), in which the liquid all flows from the inner edge to the outer edge of the packing along the radial direction. The difference among them is the moving path of gas. In the Counter-RPB, the gas flows from the outer edge to the inner edge of packing along the radial motion, while in another case the gas flows along the axial direction through the packing in the Cross-RPB. However, there is little study on Con-RPB because the gas flows in the same direction with the liquid, resulting in small relative velocity and poor mass transfer efficiency. Counter-RPB was invented firstly by Ramshaw and coworkers<sup>[21]</sup> and there was no published report concerning Counter-RPB until 1997<sup>[22]</sup>. Since the birth of rotating packed bed, the comparison of mass transfer performance between Counter-RPB and Cross-RPB has been a research hotspot. In 1997, Guo<sup>[22]</sup> firstly estimated that the height of mass transfer unit of Cross-RPB for liquid phase controlling process is 2.54 cm, which was close to that of Counter-RPB. In 2006, Lin<sup>[23]</sup> found that the height of a transfer unit (HTU) value of Cross-RPB was greater than that of Counter-RPB, and the  $k_G a_e$  value of Cross-RPB was 13—77 times higher than that of Counter-RPB in IPA absorption process. In 2008, Lin<sup>[24]</sup> reported that the overall gas volumetric mass transfer coefficients ( $k_G a_e$ ) for CO<sub>2</sub> absorption of the Cross-RPB were 2.46—2.61 times higher than those of the Counter-RPB. In the same year, Chen<sup>[25]</sup> examined the mass transfer performance of the Cross-RPB for VOCs removal, and the results showed that the mass transfer coefficient of Cross-RPB was less than that of Counter-RPB. In 2010, Jiao<sup>[26]</sup> proposed that the liquid volume mass transfer coefficient ( $k_L a_e$ ) of Cross-RPB equipped with a new structured packing was 1—2 orders of magnitude greater than that of Counter-RPB. According to these literature reports, the Cross-RPB appears to have a better mass transfer performance than the Counter-RPB for gas absorption, but the comparative standard has not been unified yet for the absorption systems, equipment sizes, and equipment structure, and furthermore, the operating conditions are different in these researches<sup>[24-26]</sup>, which would lead to some errors.

The aim of this study is to evaluate the mass transfer performance of two RPBs comprehensively with the same equipment size under the same operating conditions. Based on the previous work on the gas-liquid mass transfer, the liquid volumetric transfer coefficient  $k_L a_e$  was measured to characterize the mass transfer of RPBs in general<sup>[27-28]</sup>.

In this study, for further distinguishing the mass transfer nature of the two RPBs, the effective interfacial area,  $a_e$ , was also investigated. In addition, upon considering the energy consumption, the mass transfer effect is no longer characterized by the mass transfer coefficient only, because it should be studied with the influence of pressure drop being taken into account. Thereby the pressure drop per unit mass transfer coefficient,  $\Delta P/k_L a_e$ , was introduced to evaluate the comprehensive mass transfer performance. Intuitively, the smaller the  $\Delta P/k_L a_e$  is, the better the performance would be. The study will provide a detailed insight into the design and application of the two kinds of RPB for waste gas absorption.

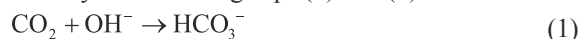
## 2 Experimental

### 2.1 Calculation

#### 2.1.1 Calculation of liquid volumetric mass transfer coefficient, $k_L a_e$

In this study, NaOH—CO<sub>2</sub> was used to measure the liquid volumetric mass transfer coefficient because the kinetics of this system is well-known and the chemicals are easy to handle.

The reaction between NaOH solution and CO<sub>2</sub> is presented by the following Eqs. (1) and (2):



The above Eq. (2) is an ionic reaction with a fast reaction rate, while Eq. (1) is carried out at a limited rate, which forms the control step. The Hatta number ( $Ha$ ) representing the ratio of chemical reaction rate to physical absorption rate in the liquid film is used to determine the rate and the type of the chemical reactions. In this study, the inlet concentration of NaOH solution was kept in the range of 0.03—0.05 mol/L and the inlet concentration of CO<sub>2</sub> was between 1% and 2%, which led to lower Hatta numbers ( $0.02 < Ha < 2$ ). In this range of Hatta number, the mass transfer process is affected by the flow pattern of the liquid, and the calculation of  $k_L a_e$  in Counter-RPB can be expressed by Eq. (3)<sup>[26, 29]</sup>:

$$k_L a_e = \frac{G_0 (y_1 - y_2)}{\pi H (r_2^2 - r_1^2) E \Delta C_m^*} \quad (3)$$

Meanwhile, due to the difference between the structure and the gas-liquid contact mode,  $k_L a_e$  in Cross-RPB can be calculated<sup>[26, 30-31]</sup> by Eq. (4):

$$k_L a_e = \frac{G_0}{\pi H (r_2^2 - r_1^2) E H_{\text{CO}_2} P} \ln(y_1 / y_2) \quad (4)$$

where, in accordance with the literature report<sup>[29]</sup>,  $E$ ,  $H_{\text{CO}_2}$ , and  $\Delta C_m^*$  can be calculated.

### 2.1.2 Calculation of effective interfacial area, $a_e$

On the basis of the calculation of  $k_L a_e$ , the inlet NaOH concentration was around 0.2–1.0 mol/L and the inlet  $\text{CO}_2$  concentration was in the range of 0.2% to 0.4%. Under such conditions, the Hatta number is greater than 2 and the chemical process is a pseudo-first-order reaction. This means that the operating conditions affecting the thickness of the liquid film can only influence the effective interfacial area, which has little effect on the mass transfer coefficient. The calculation expression of  $a_e$ <sup>[29]</sup> can be written as Eq. (5):

$$a_e = \frac{N_{\text{CO}_2}}{\sqrt{k_L D_{\text{CO}_2} H_{\text{CO}_2} P_{\text{CO}_2}}} \quad (5)$$

whereupon the methods for calculation of  $N_{\text{CO}_2}$ ,  $k_L$ ,  $D_{\text{CO}_2}$ ,  $H_{\text{CO}_2}$  and  $P_{\text{CO}_2}$  can be found in the literature<sup>[29]</sup>.

### 2.1.3 Calculation of different operating parameters

In this study, liquid spray density  $q$ , gas velocity  $u$ , and high gravity factor  $\beta$  were chosen as the major operating variables. The relevant calculation methods are shown in Eqs. (6), (7), (8), and (9).

On the basis of the gas throughput and the cross section of the packing, the gas velocity  $u$  of Cross-RPB and Counter-RPB can be calculated by Eqs. (6) and (7), respectively.

$$u = \frac{Q}{\pi(r_2^2 - r_1^2)} \quad (6)$$

$$u = \frac{Q}{\pi(r_1 + r_2)H} \quad (7)$$

in which  $Q$  is the gas volume flow rate,  $\text{m}^3/\text{h}$ , and  $r_1$  and  $r_2$  are the external and inner diameter of packing, m, respectively.

The volume of liquid spraying on the unit flow section within a unit time is the liquid spraying density  $q$ . The liquid spray density should be an appropriate value. If the liquid spray density is too small, the filler cannot be completely wetted, but if the liquid spray density is too large, liquid flooding is likely to occur, and both of these conditions will affect the gas-liquid mass transfer effect. The calculation formula can be expressed by Eq. (8).

$$q = \frac{L}{2\pi r H} = \frac{L}{\pi(r_1 + r_2)H} \quad (8)$$

where  $H$  represents the axial length of the packing, m,

and  $L$  is the liquid volume flow rate, L/h.

The high gravity factor  $\beta$  is a function of rotational speed and radius, which links the rotational speed with the radius to reduce the influence of different high gravity intensity on mass transfer effect under the same rotational speed of different equipment. The following Eq. (9) is its calculation method.

$$\beta = \frac{\omega^2 \bar{r}}{g} = \frac{\omega^2 (r_1 + r_2)}{2g} \quad (9)$$

where  $\omega$  is the rotor speed, rad/s, and  $g$  is the acceleration of gravity,  $\text{m/s}^2$ .

## 2.2 Experimental setup

Figure 1 shows the schematic diagrams of the Cross-RPB and the Counter-RPB, including packing, liquid distributor, etc.

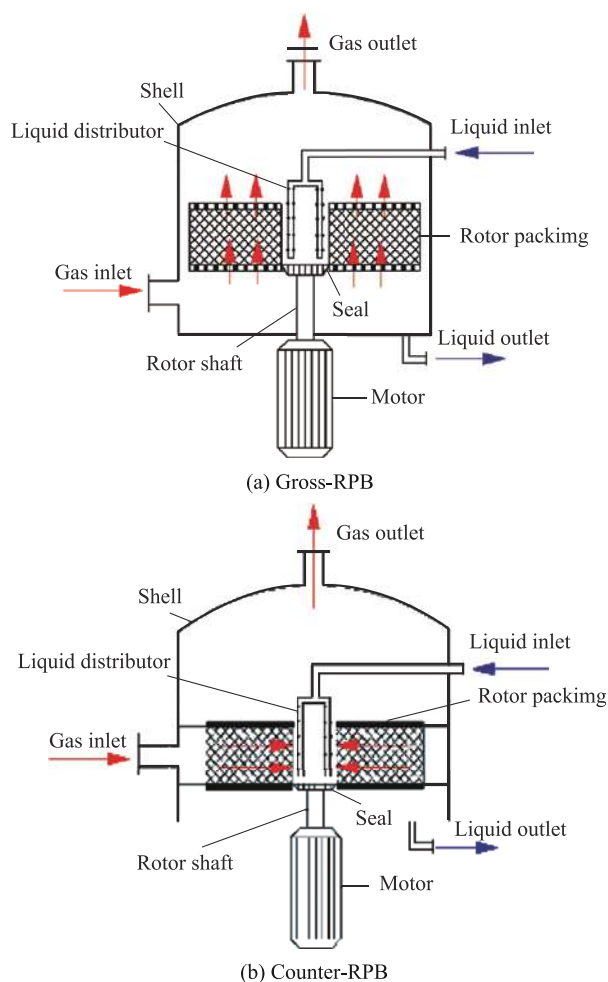


Figure 1 The sketch of Cross - and Counter-RPB

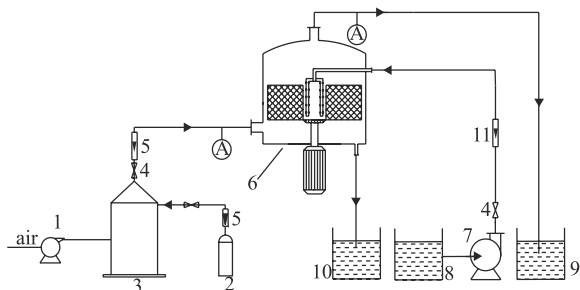
The rotor size in the two RPBs was the same, and the stainless steel mesh was chosen as the packing, with the detailed parameters given in Table 1.

**Table 1 Details of Counter-RPB and Cross-RPB**

Items	Counter-RPB	Cross-RPB
Packing zone	Stainless steel	Stainless steel
Packing type	wire mesh	wire mesh
Surface area, m <sup>2</sup> /m <sup>3</sup>	780	780
Voidage	0.95	0.95
Inner cavity zone		
Outer diameter, m	0.098	0.098
Outer cavity zone		
Outer diameter, m	0.200	0.200
Axial thickness, m	0.250	0.230

### 2.3 Experimental Procedure

Figure 2 indicates the experimental procedure for absorption of CO<sub>2</sub> by NaOH in the two RPBs. As shown in the picture, CO<sub>2</sub> and air were firstly mixed in a buffer tank, and were then introduced into the RPB through a gas pipeline. NaOH solution was pumped into the RPB through a liquid distributor and then was sprayed onto the inner edge of packing. With the aid of centrifugal force in the high gravity field, the liquid quickly moved along the radial direction to be in contact with the gas counter-currently and cross-currently in the rotated packing, respectively. Then the absorption solution was expelled from the bottom of the RPB and the gas was discharged from the top. Sampling ports were set at the inlet and outlet of gas stream to measure the concentration of the CO<sub>2</sub> with a portable CO<sub>2</sub> composite gas detector (PGM-54, RAE, USA). The double indicator method was adopted to measure the liquid concentration at the liquid inlet and the outlet. The pressure drop at the inlet and the outlet was determined by installing a U-type differential pressure gauge at relevant sampling ports.


**Figure 2 Sketch of the experimental setup**

- 1—Air blower; 2—CO<sub>2</sub> cylinder; 3—Buffer tank; 4—Valve;  
5—Gas flow meter; 6—Counter-RPB/Cross-RPB; 7—Pump;  
8—Stock tank; 9—Waste gas absorption tank;  
10—Waste liquid tank; 11—Liquid flow meter

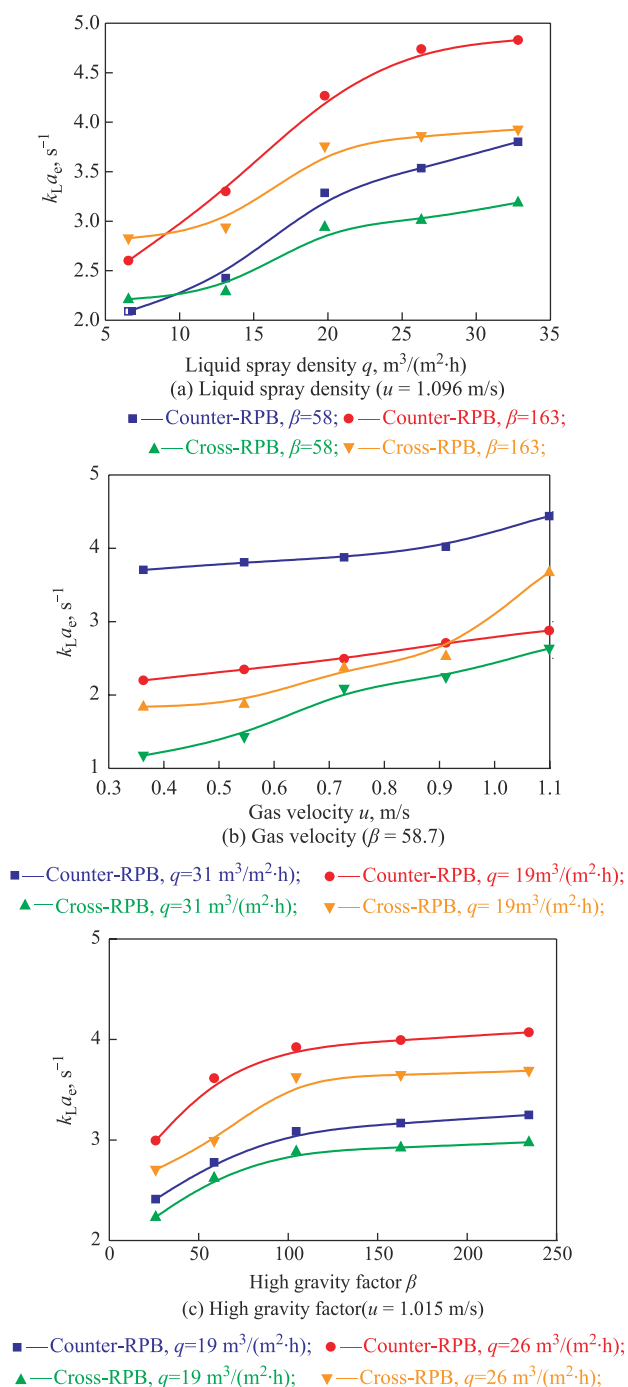
## 3 Results and Discussion

### 3.1 Liquid volumetric mass transfer coefficient, $k_L a_e$

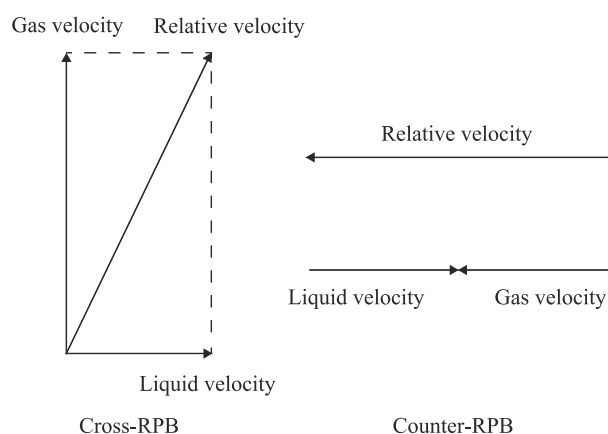
Figure 3 shows the effects of liquid spray density  $q$ , gas velocity  $u$ , and high gravity factor  $\beta$  on the liquid volumetric mass transfer coefficient  $k_L a_e$  of the Counter-RPB and the Cross-RPB. Figure 3 (a) displays the effect of liquid spray density  $q$  ranging from 6 to 32 m<sup>3</sup>/(m<sup>2</sup>·h) on the liquid volumetric mass transfer coefficient  $k_L a_e$  of the two RPBs. As shown in Figure 3 (a), it was obvious that  $k_L a_e$  firstly increased rapidly and then slowed down. The increase in liquid spray density  $q$  led to the growth in the number of liquid droplets, which would consequently increase the contact area between the gas and the liquid. However, when  $q$  continuously increased from 19 to 33 m<sup>3</sup>/(m<sup>2</sup>·h), the liquid residence time in the packing declined intensively and the action for increasing the contact area was weakened at the same time. Chen<sup>[25]</sup> also reported a similar trend of dependence of  $k_G a_e$  on liquid flow rate for absorption of VOAs. In addition, the liquid volumetric mass transfer coefficient of the Cross-RPB was less (by <20 %) than that of the Counter-RPB in this study.

Figure 3 (b) shows the effect of the gas velocity  $u$  ranging from 0.33 m/s to 1.1 m/s on the  $k_L a_e$  values of two RPBs. It can be seen from Figure 3 (b) that the liquid volumetric mass transfer coefficient  $k_L a_e$  increased with an increasing gas velocity  $u$ , and the  $k_L a_e$  curves tended to be linear. This phenomenon was also seen in previous studies<sup>[8,25]</sup>, but it took a slightly different form<sup>[24]</sup>. Each value of  $k_L a_e$  in the Counter-RPB under the same operating conditions was always higher than that in the Cross-RPB. This outcome might be caused by the fact that the countercurrent flow could provide a larger relative velocity between liquid and gas, which made the collision between gas and liquid in Counter-RPB more violent than that in Cross-RPB, which could be easily described in Figure 4. The gas flowing in the Counter-RPB moved mainly in the radial direction, while in another case, the gas flowed along the axial direction in the Cross-RPB, leading to a greater relative velocity of the gas and the liquid in the Counter-RPB, as compared to that

in the Cross-RPB. It is also found that the change of  $k_L a_e$  in the Cross-RPB ( $1.6 \text{ s}^{-1}$ ) was more than that in the Counter-RPB ( $0.7 \text{ s}^{-1}$ ), which demonstrated that the influence of gas velocity on the Cross-RPB was more significant than that on the Counter-RPB, and the different flow path could lead to different mass transfer characteristics.



**Figure 3 Comparison of volumetric mass-transfer coefficient between Counter-RPB and Cross-RPB**



**Figure 4 Relative velocity provided by Cross-RPB and Counter-RPB**

Figure 3(c) illustrates that  $k_L a_e$  is a function of high gravity factor  $\beta$  ranging from 26 to 240. It can be seen from Figure 3(c) that the  $k_L a_e$  increased with an increasing high gravity factor  $\beta$  and then reached its highest value when the high gravity factor  $\beta$  was around 104. Reason for this phenomenon is the effect of centrifugal and shear force formed from rotated packing on the liquid flow which increased with the increase of  $\beta$ , and consequently the liquid fed by the distributor was immediately broken into droplets and threads in the internal of packing, and thin films on the packing, which was beneficial to the increase of the gas-liquid contact area. Although the high gravity factor continued to increase, the liquid volume was limited, which led to a slight increase of  $k_L a_e$  at the high value of  $\beta$ . Jiao, et al.<sup>[26]</sup> also demonstrated the similar variation of  $k_L a_e$  which was dependent on  $\beta$ . Besides, the  $k_L a_e$  of Counter-RPB was approximately 1.18—1.37 times more than that of Cross-RPB under the same operating conditions, which demonstrated that  $k_L a_e$  was impacted by the flow pattern established in the system. Besides, the optimal high gravity factor should be around 104 as depicted by Figure 3(c).

To identify mass transfer performance of the Cross-RPB and the Counter-RPB, the  $k_L a_e$  values obtained by this work and previous studies are listed in Table 2. It can be clearly seen from Table 2 that the  $k_L a_e$  value in the Counter-RPB was mostly higher than that in the Cross-RPB, indicating that the Counter-RPB showed superior



mass transfer characteristics.

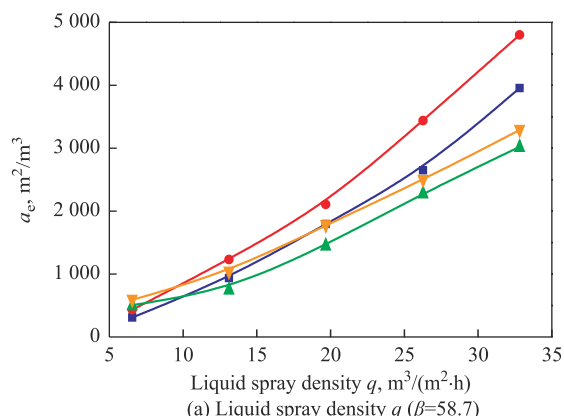
**Table 2 Comparison of mass transfer coefficients in Counter-RPB and Cross-RPB**

Researchers	$k_1 a_e, s^{-1}$	
	Counter-RPB	Cross-RPB
[24]	0.74—1.72	0.30—0.66
[25]	3.00—10.00	0.30—3.90
[26]	0.10—0.15	0.28—1.33
Present work		1.13—4.05

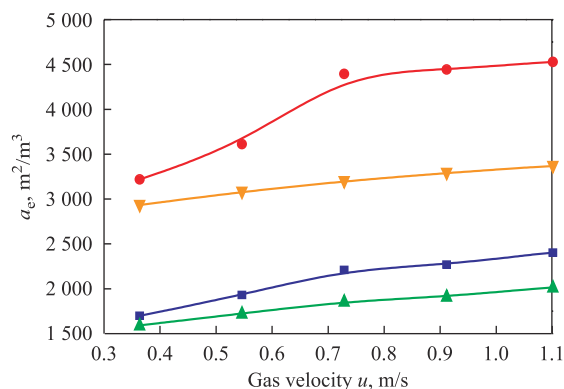
### 3.2 Effective interfacial area, $a_e$

Figure 5(a)–(c) shows the effects of liquid spray density  $q$ , gas velocity  $u$ , and high gravity factor  $\beta$  on the effective interfacial area  $a_e$  in the Counter-RPB and the Cross-RPB. It was found that the effective interfacial area  $a_e$  increased with an increasing liquid spray density  $q$ , gas velocity  $u$ , and high gravity factor  $\beta$ , as evidenced by the curves of Figure 5(a)–(c), which was similar to the trends shown in Figure 3(a)–(c). It explained that RPBs offered mass-transfer intensification through increasing the effective interfacial area. It can be also seen from Figure 5 that the extent of change of  $\Delta a_e$  was different:  $\Delta a_e$  for  $u$  was between 548.1  $m^2/m^3$  and 1 149.4  $m^2/m^3$ ,  $\Delta a_e$  for  $\beta$  was between 422.2  $m^2/m^3$  and 1 316.4  $m^2/m^3$ , while  $\Delta a_e$  for  $q$  was in the range of 2 438.6  $m^2/m^3$  to 4 202.1  $m^2/m^3$ , which means that the liquid spray density  $q$  greatly influenced the  $a_e$ , as compared with the influence of gas velocity  $u$  and high gravity factor  $\beta$ . Most importantly, the effective interfacial area  $a_e$  of the Counter-RPB was almost higher than that of the Cross-RPB under the same operating conditions. For a better explanation of this phenomenon, three interactions between gas, liquid, and packing participating in mass transfer process in RPB are displayed in Figure 6. Due to the same operating conditions, the interaction between gas/packing and liquid/packing should be similar in the Counter-RPB and the Cross-RPB, but it was apparent that the mode of contact between the liquid and gas was different and the countercurrent flow in RPB could provide a higher

relative velocity, resulting in more violent collision and dispersion that were beneficial to enlargement of  $a_e$ . Thereby, it was realized that the effective interfacial area  $a_e$  was impacted by the pattern in which the flows were established as well.



(a) Liquid spray density  $q$  ( $\beta=58.7$ )



(b) Gas velocity  $u$  ( $\beta=58.7$ )

(c) High gravity factor  $\beta$  ( $u=0.91$  m/s)

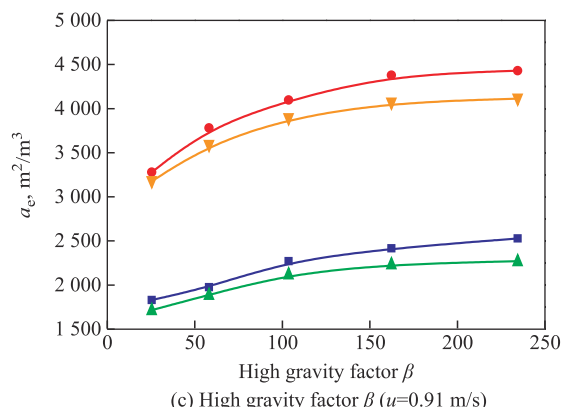


**Figure 5 Comparison of effective interfacial area  $a_e$  between Counter-RPB and Cross-RPB**

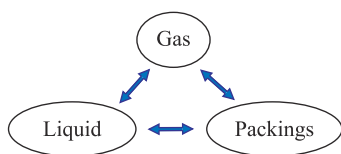


Figure 6 Three interactions of mass transfer process in an RPB

### 3.3 The mass-transfer comprehensive comparison

In order to evaluate the comprehensive performance of rotating packed bed, the energy consumption is taken into account.  $\Delta P/k_L a_e$  meaning how much energy is needed to produce a unit mass transfer was adopted to evaluate the effect of operating parameters on the comprehensive characteristics of mass transfer<sup>[26]</sup>.

As is shown in Figure 7, the  $\Delta P/k_L a_e$  of the Counter-RPB increased with the increase of gas velocity  $u$ , and the maximum value of  $\Delta P/k_L a_e$  in the Cross-RPB was observed at 0.84 m/s. Because of the different increment of  $\Delta P$  and  $k_L a_e$  of the two RPBs, the Counter-RPB demonstrated low  $\Delta P/k_L a_e$  when the gas velocity was less than 0.71 m/s, while it was exactly reversed when the gas velocity was more than 0.71 m/s. It could be inferred that the Counter-RPB is more suitable for the small gas velocity treatment, while the Cross-RPB is suitable for the large gas velocity treatment. Figure 7(b) illustrates that  $\Delta P/k_L a_e$  increased with an increasing high gravity factor  $\beta$  in two RPBs, and  $\Delta P/k_L a_e$  of the Counter-RPB changed slightly when the  $\beta$  value was above 100, while  $\Delta P/k_L a_e$  of the Cross-RPB increased notably from 30 Pa·s to 50 Pa·s. Besides,  $\Delta P/k_L a_e$  value of the Counter-RPB was higher than that of the Cross-RPB under the same operating conditions. Figure 7(c) shows that  $\Delta P/k_L a_e$  decreased with the increase of liquid spray density  $q$  in two RPBs, and the decrement in Counter-RPB was more than that in Cross-RPB. The values of  $\Delta P/k_L a_e$  in the Counter-RPB were by about 23—66 Pa·s higher than those of Cross-RPB. On the basis of the results obtained thereby, the Cross-RPB had a superior comprehensive performance to cope with large gas velocity, while the Counter-RPB had a superior comprehensive performance to cope with small gas velocity, which means that the Cross-RPB would have a great potential for industrial scale-up applications.

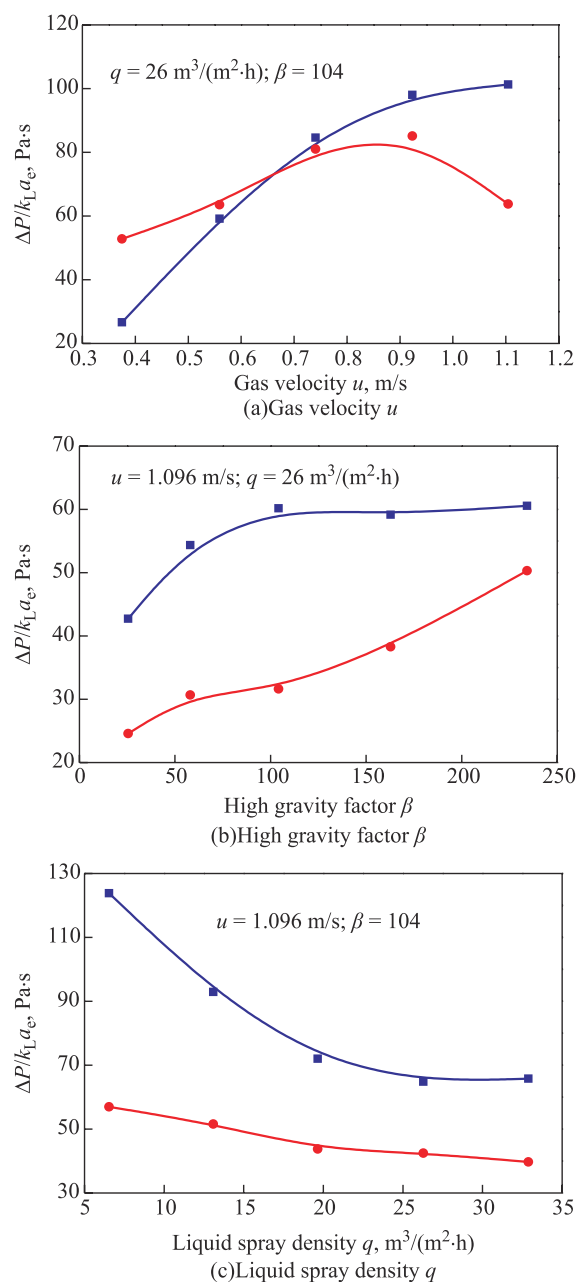


Figure 7 Comparison of  $\Delta P/k_L a_e$  between Counter-RPB and Cross-RPB

■—Counter-RPB; ●—Cross-RPB

### 3.4 Empirical correlations

The correlations of mass transfer coefficient were proposed while taking into consideration the different operating parameters, packing structures, types of RPB, and the experimental system. Eq. (10) is assumed to be comprised of the following parameters,  $Re_G$ ,  $We_L$ , and  $G_a$ :

$$k_L a_e = A Re_G^a We_L^b G_a^c \quad (10)$$

in which  $A$ ,  $a$ ,  $b$ , and  $c$  are undetermined coefficients.

$Re_G$  is related to gas flow rate, material quality, structure of packing, rotating packed bed, etc. And  $We_L$  and  $G_a$  can reflect the liquid flow rate, high gravity fields, surface tension, reaction system, etc. After making regression of the experimental data, the empirical correlations for Counter-RPB and Cross-RPB can be obtained with MATLAB program, respectively, as shown in Eqs. (11) and (12).

For Cross-RPB:

$$k_L a_e = 1.2214 Re_G^{0.57921} We_L^{0.05417} G_a^{0.20032} \quad (11)$$

For Counter-RPB:

$$k_L a_e = 7.389 Re_G^{0.19458} We_L^{0.39398} G_a^{0.11926} \quad (12)$$

Figure 8 shows the comparison between the experimental data and the calculated data. The relative errors were within  $\pm 5\%$  and the correlation coefficients obtained by the regression analysis were above 0.99, denoting that the correlation could describe the phenomenon well.

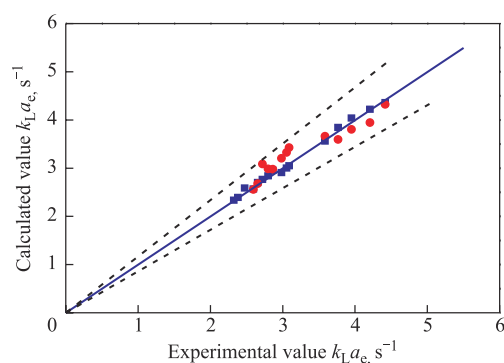


**Figure 8 Comparison between experimental value and calculated value of liquid volumetric mass transfer coefficient  $k_L a_e$**   
 ■—Counter-RPB; ●—Cross-RPB; - - -  $\pm 5\%$

## 4 Conclusions

In this work, the mass transfer characteristics of the Counter-RPB and the Cross-RPB with similar equipment sizes were compared under the same operating conditions. The volumetric mass transfer coefficient  $k_L a_e$  and the effective interfacial area  $a_e$  were measured. In order to make comprehensive comparison on mass transfer,  $\Delta P/k_L a_e$  was adopted.

Experimental results indicated that the values of  $k_L a_e$  and  $a_e$  increased with an increasing liquid spray density  $q$ , gas velocity, and high gravity factor  $\beta$ . It also found that  $k_L a_e$  and  $a_e$  were deeply affected by liquid spray density  $q$  and gas velocity  $u$ , while the high gravity factor  $\beta$  had little effect on them. The volumetric mass transfer coefficient

$k_L a_e$  of the Counter-RPB was higher than that of the Cross-RPB, and the effective interfacial area  $a_e$  of the Counter-RPB was almost larger than that of the Cross-RPB under the same operating parameters, which indicated that the Counter-RPB usually demonstrated better mass transfer characteristics. However, upon considering the energy consumption, the Counter-RPB had higher  $\Delta P/k_L a_e$  than the Cross-RPB when the gas velocity was less than 0.71 m/s, but the consequence was reversed when the gas velocity was higher than 0.71 m/s, which could infer that the Counter-RPB was more suitable for the small gas velocity treatment, while the Cross-RPB was suitable for the large gas velocity treatment. The relative error of experimental value to the calculated value of  $k_L a_e$  was less than 5%. In summary, the mass transfer characteristic of RPB was deeply impacted by the manner in which the flows were established, and the Cross-RPB would have a great potential for industrial scale-up applications.

**Acknowledgements:** The study is supported by the National Key R & D Program of China: The ultra-low emission control technology for coal-fired industrial boilers (2016YFC0204103), and the Provincial Key R&D Program of Shanxi: R&D of the coal-fired industrial boiler smoke ultra-low emission technology and equipment (201703D111018).

## References

- [1] Kang J L, Sun K, Wong D S H, et al. Modeling studies on absorption of  $CO_2$  by monoethanolamine in rotating packed bed[J]. International Journal of Greenhouse Gas Control, 2014, 25: 141-150
- [2] Lin C C, Chen B C. Carbon dioxide absorption in a cross-flow rotating packed bed[J]. Chemical Engineering Research & Design, 2011, 89(9): 1722-1729
- [3] Lin C C, Chen Y W. Performance of a cross-flow rotating packed bed in removing carbon dioxide from gaseous streams by chemical absorption[J]. International Journal of Greenhouse Gas Control, 2011, 5(4): 668-675
- [4] Sheng M P, Sun B C, Zhang F M, et al. Mass-transfer characteristics of the  $CO_2$  absorption process in a rotating packed bed[J]. Energy & Fuels, 2016, 30(5): 4215-4220
- [5] Guo K, Wen J W, Zhao Y, et al. Optimal packing of a rotating packed bed for  $H_2S$  removal[J]. Environmental Science & Technology, 2014, 48(12): 6844-6849



- [6] Bai S, Chu G W, Li S C, et al. SO<sub>2</sub> Removal in a pilot scale rotating packed bed[J]. Environmental Engineering Science, 2015, 32(9): 806-815
- [7] Li W Y, Wu W, Zou H K, et al. Process intensification of VOC removal from high viscous media by rotating packed bed[J]. Chinese Journal of Chemical Engineering, 2009, 17(3): 389-393
- [8] Lin C C, Lin Y C, Chien K S. VOCs absorption in rotating packed beds equipped with blade packing[J]. Journal of Industrial and Engineering Chemistry, 2009, 15(6): 813-818
- [9] Gao Jing, Yan Junjuan, Liu Youzhi, et al. Phenol wastewater degradation by electrocatalytic oxidation with RuO<sub>2</sub>-IrO<sub>2</sub>-SnO<sub>2</sub>/Ti anodes in the high gravity field[J]. China Petroleum Processing & Petrochemical Technology, 2018, 20(4): 75-81
- [10] Modak J B, Bhowal A, Datta S. Extraction of dye from aqueous solution in rotating packed bed[J]. Journal of Hazardous Materials, 2016, 304: 337-342
- [11] Panda M, Bhowal A, Datta S. Removal of hexavalent chromium by biosorption process in rotating packed bed[J]. Environmental Science & Technology, 2011, 45(19): 8460-8466
- [12] Zeng Z Q, Zou H K, Li X, et al. Degradation of phenol by ozone in the presence of Fenton reagent in a rotating packed bed[J]. Chemical Engineering Journal, 2013, 229: 404-411
- [13] Zhao H, Shao L, Chen J F. High-gravity process intensification technology and application[J]. Chemical Engineering Journal, 2010, 156(3): 588-593
- [14] Jiang X P, Liu Y Z, Gu M D. Absorption of sulphur dioxide with sodium citrate buffer solution in a rotating packed bed[J]. Chinese Journal of Chemical Engineering, 2011, 19(4): 687-692
- [15] Li X P, Liu Y Z. Characteristics of fin baffle packing used in rotating packed bed[J]. Chinese Journal of Chemical Engineering, 2010, 18(1): 55-60
- [16] Li Y, Liu Y Z, Zhang L Y, et al. Absorption of NO<sub>x</sub> into nitric acid solution in rotating packed bed[J]. Chinese Journal of Chemical Engineering, 2010, 18(2): 244-248
- [17] Zheng C, Guo K, Feng Y, et al. Pressure drop of centripetal gas flow through rotating beds[J]. Industrial & Engineering Chemistry Research, 2000, 39(3): 829-834
- [18] Lin C C, Chen B C. Characteristics of cross-flow rotating packed beds[J]. Journal of Industrial and Engineering Chemistry, 2008, 14(3): 322-327
- [19] Ramshaw C. HIGEE distillation—An example of process intensification[J]. Chem Engr, 1983, 389: 13-14
- [20] Stankiewicz A I. Process intensification: Transforming chemical engineering[J]. Chemical Engineering Progress, 2000, 96: 22-33
- [21] Ramshaw C, Mallison R H. Mass transfer process: The United States, US4283255[P]. 1981-08-11
- [22] Guo F, Chong Z, Kai G, et al. Hydrodynamics and mass transfer in cross-flow rotating packed bed[J]. Chemical Engineering Science, 1997, 52(21/22): 3853-3859
- [23] Lin C C, Wei T Y, Hsu S K, et al. Performance of a pilot-scale cross-flow rotating packed bed in removing VOCs from waste gas streams[J]. Separation and Purification Technology, 2006, 52(2): 274-279
- [24] Lin C C, Chen B C, Chen Y S, et al. Feasibility of a cross-flow rotating packed bed in removing carbon dioxide from gaseous streams[J]. Separation & Purification Technology, 2008, 62(3): 507-512
- [25] Chen Y S, Hsu Y C, Lin C C, et al. Volatile organic compounds absorption in a cross-flow rotating packed bed[J]. Environmental Science & Technology, 2008, 42(7): 2631-2636
- [26] Jiao W Z, Liu Y Z, Qi G S. Gas pressure drop and mass transfer characteristics in a cross-flow rotating packed bed with porous plate packing[J]. Industrial & Engineering Chemistry Research, 2010, 49(8): 3732-3740
- [27] Luo Y, Chu G W, Zou H K, et al. Mass transfer studies in a rotating packed bed with novel rotors: Chemisorption of CO<sub>2</sub>[J]. Industrial & Engineering Chemistry Research, 2012, 51(26): 9164-9172
- [28] Luo Y, Chu G W, Zou H K, et al. Gas-liquid effective interfacial area in a rotating packed bed[J]. Industrial & Engineering Chemistry Research, 2012, 51(50): 16320-16325
- [29] Liu Y Z, Gu D Y, Xu C C, et al. Mass transfer characteristics in a rotating packed bed with split packing[J]. Chinese Journal of Chemical Engineering, 2015, 23(5): 868-872
- [30] Chu G W, Luo Y, Xing Z Y, et al. Mass-transfer studies in a novel multiliquid-inlet rotating packed bed[J]. Industrial & Engineering Chemistry Research, 2014, 53(48): 18580-18584
- [31] Fang Jing, Cheng Xiaomin, Li Xiaochun, et al. Shortcut method of design and energy-saving analysis of sargent dividing wall column[J]. China Petroleum Processing & Petrochemical Technology, 2018, 20(4): 99-108